Available online at www.sciencedirect.com
ScienceDirect
Progress in Natural Science 19 (2009) 861–872
Progress in Natural Science
www.elsevier.com/locate/pnsc

Use of a multi-temporal grid method to analyze changes in glacier coverage in the Tibetan Plateau

Qinghua Ye [a,b,*], Feng Chen [a], Alfred Stein [c], Zhenwei Zhong [a]

[a] *Laboratory of Tibetan Environment Changes and Land Surface Processes, Institute of Tibetan Plateau Research, Chinese Academy of Sciences (CAS), Beijing 100085, China*
[b] *State Key Laboratory of Remote Sensing Science, Institute of Remote Sensing Applications of CAS, Beijing 100101, China*
[c] *International Institute for Geo-Information Science and Earth Observation (ITC), PO Box 6, 7500 AA Enschede, The Netherlands*

Received 23 June 2008; received in revised form 20 November 2008; accepted 11 December 2008

Abstract

This paper describes a multi-temporal grid method for quantifying changes in glacier coverage. A multi-temporal grid synthesizes spatial, attribute and process components of glacier information by sequentially combining spatial data from satellite images or maps. It enables us to identify glacier retreat and advance areas in individual grid cells for three or more periods of data sets. Discrepancies among the sequential data sets were detected graphically and numerically, including noise from geo-location error, misclassification, or different interpretation results in various pixel resolutions. Noise was detected and corrected to a large extent by visualization of the synthetic grid. The paper compares the results with that from a common method based on individual data sets, focusing on the Mt. Naimona'Nyi and Mt. Qomolangma regions at the northern slopes of the Himalayas. Results show that the identified noise (e.g. by 2.5 km^2 in the Mt. Naimona'Nyi region) is much larger than measurement uncertainty calculated by sensor resolution and co-registration error (e.g. by 0.015 km^2 in the Mt. Naimona'Nyi region). After noise removal, we notice that glacier recession clearly accelerates. The multi-temporal grid method results in a better quantification of glacier variation. It shows that glaciers in the Himalayas have both retreated and advanced during the last several decades, with retreat dominating and accelerating. Glaciers on the northern slope of Mt. Qomolangma in the middle Himalayas retreat more extensively and faster than those in the Mt. Naimona'Nyi region in the western Himalayas.

Keywords: Glacier; Multi-temporal grid; Mt. Naimona'Nyi; Mt. Qomolangma; Himalayas; Tibetan Plateau

1. Introduction

Remote sensing satellite techniques, including microwave data and optical imagery have been frequently applied in surveys for Alpine glaciers. The reason for this successful application is that glaciers are clearly distinguishable by satellite sensors from their background and that they are difficult to access. Landsat imagery is a primary data source for glaciological research [1–3], providing glacier information in remote areas since 1972 [4]. More recently, the Advanced Space-borne Thermal Emission and Reflection Radiometer (ASTER), with 15 m resolution Visible Near-infrared (VNIR) bands and an along-track stereo imaging capability [5], is widely used for assessment of glacier dynamics. One example concerns the Global Land Ice Measurements from Space (GLIMS) project [6–8].

Common methods of research on variation in glacier distribution by remote sensing focus on extraction of glacier

* Corresponding author. Tel.: +86 10 62849397; fax: +86 10 62849886.
E-mail address: yeqh@itpcas.ac.cn (Q. Ye).

1002-0071/$ - see front matter © 2009 National Natural Science Foundation of China and Chinese Academy of Sciences. Published by Elsevier Limited and Science in China Press. All rights reserved.
doi:10.1016/j.pnsc.2008.12.002

information from individual multi-spectral satellite images by various methodologies. A distinction is made into manual digitization [1,9–11] and automatic algorithms such as the bands algebraic operation and multi-spectral classification, for example the Normalized Difference Snow Index (NDSI) [12,13], the spectral-band ratio [14–17] and unsupervised or supervised classification techniques [18,19]. Traditional methods tend to use individual images from different epochs for glacier delineation, compare the length of glacier termini or quantity of glacier areas from individual data sets and visualize the combined results by overlaying vector–vector data in a map or vector-raster format [1,11,20]. Such methods, however, do not consider noise, which may lead to discrepancies or inconsistencies and that is difficult to identify from individual images only. Common causes for noise are the use of different data sources, geo-location errors, co-registration errors, misclassification from individual images due to different methods, principles in glacier delineation, or varying definitions of what to include as the "glacier" [21], uncertainties from manual mapping of debris-covered ice, regions in cast shadow or differences in perennial snow cover that are attached to a glacier. Such discrepancies have an effect on classification from different data sources such as satellite images, aerial photographs, topographical maps and historical maps when optimizing the temporal research scope [11,22]. In this study, we used the multi-temporal grid method to account for map variation in regional glacier distribution.

The aim of this paper is to report the uncertainty of glacier changes in area measurement by comparing the usual classification results from individual data sets with that of the multi-temporal grid method. The study focuses on the Mt. Naimona'Nyi and Mt. Qomolangma regions in the Himalayas in China. The results, their uncertainty and the eliminated noises in the two regions are presented, compared and discussed.

2. Research area

Recently, pronounced glacier retreat, with strong regional variability, has been observed in the Himalayas and the Tibet plateau [23–32]. This study considers two regions in the northern Himalayas: the Mt. Naimona'Nyi, the highest peak of the south-western Himalayan Mountains, 81°00′E–81°47′E; 30°04′N–31°16′N (Fig. 1) and the northern slope of Mt. Qomolangma, also known as Mt. Everest, located in the middle Himalayan Mountains, 27°59′–28°11′N and 86°44′–86°59′E (Fig. 1).

2.1. Mt. Naimona'Nyi region

Changes of glacier coverage in the Mt. Naimona'Nyi region were surveyed by using a series of digital images (Table 1), 1:50,000 topographic maps from aerial photographs acquired in 1974 and a 1:50,000 Digital Elevation Model (DEM, with 20 m equidistant contour lines and 25 m cell size), surveyed and mapped by the State Bureau of Surveying and Mapping in China. Uplands consisting of moraines were left from the retreat of ancient glaciers in the Mt. Naimona'Nyi region. The termini of modern glaciers are at approximately 5400 m elevation, with a segment of glacier that is most likely debris-covered in the

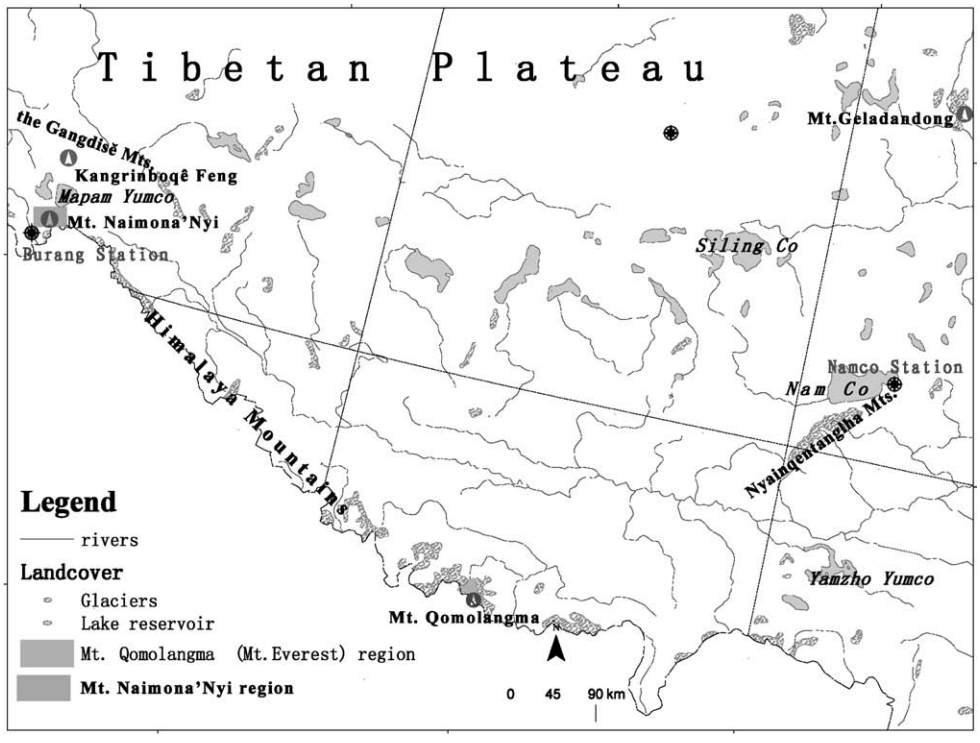

Fig. 1. Location of the Mt. Naimona'Nyi and Mt. Qomolangma regions on the Tibetan Plateau.

Table 1
Digital satellite images used in the paper.

Region	Sensor	Date	Path/row	Pixel size (VNIR, m)	Solar azimuth	Solar elevation
Mt. Naimona'Nyi region	Landsat2 MSS	6 December 1976	155/39	57.00	146.27	29.36
	Landsat5 TM	23 October 1990	144/39	28.50	142.00	40.00
	Landsat7 ETM+	9 November 1999	144/39	28.50	155.20	39.20
	Terra ASTER	3 October 2003		14.25	155.17	52.56
	Terra ASTER	3 October 2003		14.25	154.70	52.86
	ALOS/AVNIR-2	9 September 2007		10.00	143.57	60.34
Mt. Qomolangma region	Landsat2 MSS	19 December 1976	150/41	57.00	144.03	29.76
	Landsat5 TM	11 November 1992	140/41	28.50	147.00	37.00
	Landsat7 ETM+	30 October 2000	140/41	28.50	151.09	43.94
	Terra ASTER	23 October 2003		14.25	158.65	48.60

south (Fig. 2(a)–(d)). According to meteorological data from the Burang Station (3900 m a.s.l., Fig. 1) the average annual mean air temperature increased by 0.8 °C during the period from 1973 to 2004 [33]. The average annual precipitation decreased by 38 mm from 169.3 mm in 1973–1990 to 131.3 mm in 1990–1999, then increased slightly to 144.0 mm in 1999–2003.

2.2. Mt. Qomolangma region

Change of glacier coverage in the Rongbuk river catchment on the northern slope of Mt. Qomolangma in the middle Himalayas (hereafter called the Mt. Qomolangma region) was studied using a series of digital images (Table 1), 1:50,000 topographic maps produced from aerial photographs acquired in 1974 and 1:50,000 DEM. Research focused on a 280 km^2 area with altitudes from 5120 m to 8844 m a.s.l. The Rongbuk River is fed by the Rongbuk glacier, the largest glacier in the catchment with three major branches, named the east, the middle, and the west Rongbuk glacier, respectively. The existence of a debris-covered terminus and glacier lakes of the Rongbuk glacier makes conditions complex (Fig. 2e and f). At the snow line (from approximately 5800 to 6200 a.s.l.) on the northern slope of Mt. Qomolangma, average annual precipitation was between 500 and 800 mm and mean temperatures between −4 and −9 °C [34]. The main water supply in precipitation is from the Indian Ocean monsoon and local circulations [35].

As changes of the debris-covered terminus were hard to discern from multi-spectral images, we used the ultimate serac as the glacier terminus in the Mt. Qomolangma region. This research did not include the debris-covered glaciers/terminus in the two regions, which was not dominant in the area.

3. Methodology

3.1. DEM evaluation

The raw digital satellite images (e.g. ASTER and ALOS/AVNIR-2 data) have to be accurately orthorectified using a DEM and coregistered using topographic maps before glacier coverage change detections based on pixels. For the Mt. Qomolangma region, the horizontal accuracy of DEM is within 1.0 grid cell, i.e., 25 m of the 1:50,000 topographic map of the region. The height accuracy of DEM was evaluated by comparing 344 elevation check points on the 1:50,000 topographic maps with the corresponding height values for the same locations in the DEM. We obtained an average height difference of 13.3 m, with a standard deviation of 18.2 m. Residual root-mean-square error (RMSE) [36] of the DEM with respect to the topographic map is 26.1 m, with maximum height deviations equaling −108.8 and +36.3 m. For the Mt. Naimona'Nyi region, the accuracy of the DEM was also evaluated; its RMSE with respect to the topographic map is 20.93 m [37]. Ortho-rectification accuracy in the two regions was within one pixel. All image data were converted from different sources to a common format defined in Arc/Info with Transverse Mercator projection and Krasovsky1940 spheroid. Precise co-registration for all ortho-images was based on the 1:50,000 topographic maps, which were used as the common base. All co-registration errors were within 25 m.

3.2. Glacier classifications

To improve the contrast between the glacier ice and surrounding areas on ALOS/AVNIR-2 images, false color composite images were constructed in this study using bands 4 (0.76–0.89 μm), 3 (0.61–0.69 μm), and 2 (0.52–0.60 μm). Glaciers were mapped by a supervised classification, followed by removal of cloud-covered non-glacierized areas by manual editing. Glacier classifications from other images in the Mt. Naimona'Nyi study region followed the methods described by Ye and others [37]. Glacier classifications from all individual images in the Mt. Naimona'Nyi region are shown in Fig. 3. In the Mt. Qomolangma region, the 1976 Landsat MSS image was not used because of the big mountain shade in the image. Glaciers with terminus at seracs on the 1:50,000 scale topographic maps and sequential Landsat images were mapped from the false color image by on-screen digitizing with manual delineation in the Arc/Info software. The accuracy of manual digitization was controlled within 25 m.

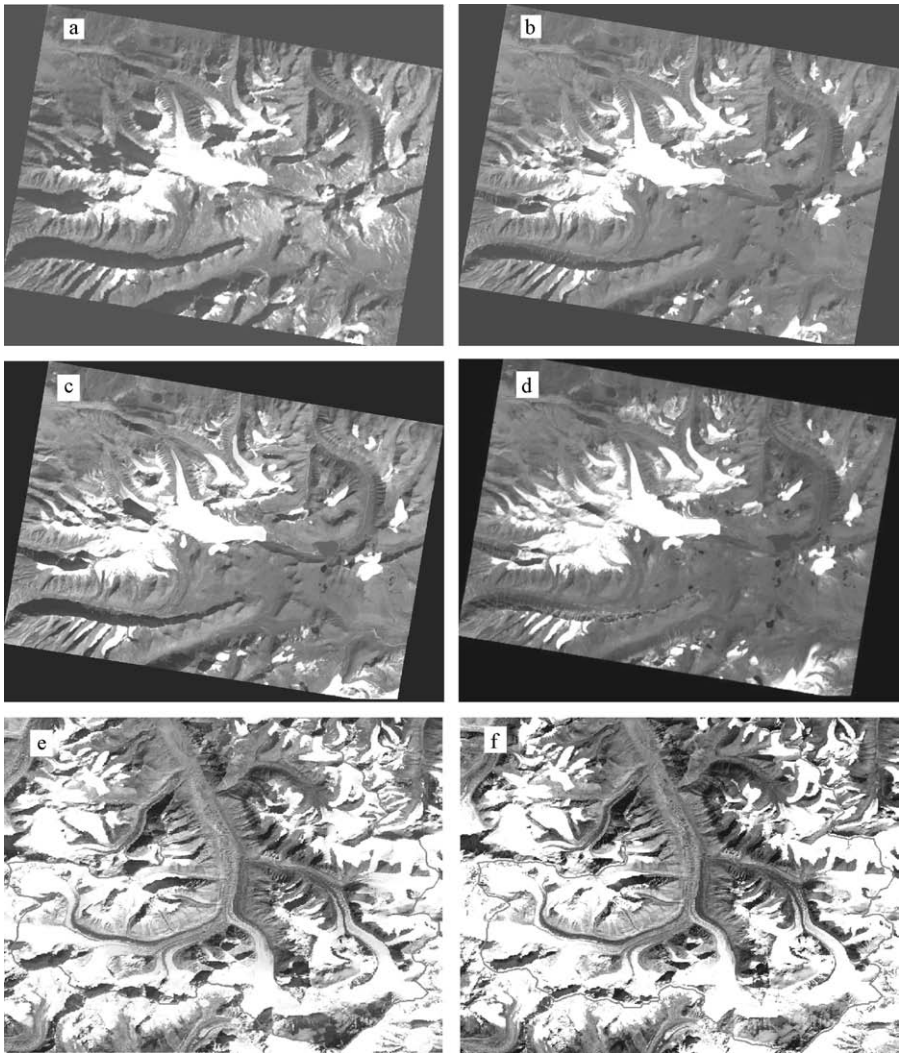

Fig. 2. Digital satellite images used in Mt. Naimona'Nyi (a–d) and Mt. Qomolangma (e and f) regions. (a) Landsat MSS digital image in 1976 (RGB:421); (b) Landsat TM digital image in 1990 (RGB:432); (c) Landsat TM digital image in 1999 (RGB:432); (d) ASTER digital image in 2003 (RGB:3N21); (e) Landsat TM digital image in 2000 (RGB:432); (f) ASTER digital image in 2003 (RGB:3N21).

Glacier classifications from all individual images were recoded by assigning the value 5 to the non-glacierized area or the value 7 to the glacier area. The choice of these values is somewhat arbitrary, as, in fact, any other two different one-digit values might have been used here as well, which would allow attribute data from different epochs to be involved in subsequent calculations. This classification scheme facilitates the algebraic operations among classification results from individual images from the Arc/Info Grid module. So far, traditional studies of glacier variation using remote sensing would be complete with data interpretation and a comparison of the classification results from sequential individual data sets [1,5,11,17].

3.3. The multi-temporal grid method

Based on the usual method for glacier classification, we developed a multi-temporal grid method for studying coverage of glacier changes by means of GIS and remote sensing techniques [38]. It is an application of the geo-information Tupu (Carto-methodology in Geo-information, CMGI) [39–41], which is a combination of geospatial dynamics and temporal analysis based on a grid unit [42]. We used the 30 m grid cell as the basic unit, i.e., all glacier classification results from individual images were re-sampled to the same pixel size by 30 m grid cell resolution. Discrete grid cells of a fixed resolution are suitable for spatial and temporal analysis of large quantities of data in GIS. We consider a variable of $P_{i,k}(x,y)$ that expresses the attribute feature P_i, $i = 1, \ldots, m$, at sampling time T_k and spatial position $S_k(x_k, y_k)$ for $k = 1, \ldots, n$. Synthesized by a temporal map algebra, the multi-temporal grid unit has all the sequential attribute information within the study area. It is a synthesis of glacier characteristics of "space· attribute· process" and is fundamental to providing insights into spatial and temporal dynamics of transition sequences [42]. The unit in the series of multi-temporal grids is similar to the geographic unit, which could also

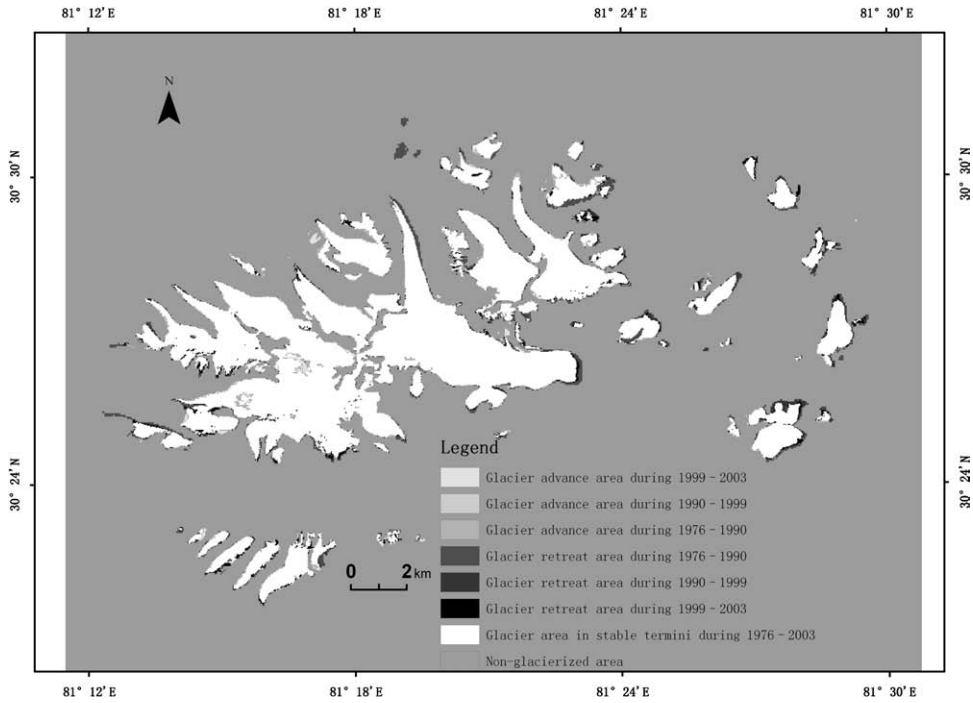

Fig. 3. Glacier coverage changes in the Mt. Naimona'Nyi region during 1976–2003.

be classified into a series of multi-categories at multi-grades and multi-scales. The multi-grades of categories of grid units could be set up by synthesis and classification according to spatial–temporal scales, research objectives and given principles.

The attribute values equal to 5 and 7 for each grid cell were combined over time using the classification results from the four images: the 1976, 1990, 1999, and 2003 images in the Mt. Naimona'Nyi region and the 1974, 1992, 2000 and 2002 images in the Mt. Qomolangma region by map algebra in the Arc/Info Grid module (Eqs. (1) and (2)). This generated a multi-temporal grid with a four-digit value in each grid cell. This step enabled us to track spatial–temporal glacier coverage changes in each grid cell during the corresponding period.

$$\mathrm{Nyi_G} = \mathrm{Nyi_{76}} \times 10^3 + \mathrm{Nyi_{90}} \times 10^2 + \mathrm{Nyi_{99}} \times 10 + \mathrm{Nyi_{03}}, \quad (1)$$

where $\mathrm{Nyi_G}$ is the multi-temporal grid value on glacier variation during 1976–2003 in the Mt. Naimona'Nyi region, and $\mathrm{Nyi_{76}}$, $\mathrm{Nyi_{90}}$, $\mathrm{Nyi_{99}}$, and $\mathrm{Nyi_{03}}$ are the classification results of glacier coverage from the images of 1976, 1990, 1999, and 2003, respectively. Similarly,

$$\mathrm{Qomo_G} = \mathrm{Qomo_{74}} \times 10^3 + \mathrm{Qomo_{92}} \times 10^2 + \mathrm{Qomo_{00}} \times 10 + \mathrm{Qomo_{03}}, \quad (2)$$

where Glacier_Qomo is the multi-temporal grid value on glacier variation in the Mt. Qomolangma region during the 1974–2003 period and $\mathrm{Qomo_{74}}$, $\mathrm{Qomo_{92}}$, $\mathrm{Qomo_{00}}$ and $\mathrm{Qomo_{03}}$ are the glacier coverage from the images or maps of 1974, 1992, 2000 and 2003, respectively, obtained by manual digitization.

3.4. Principles to distinguish real glacier changes and noises

Various types of glacier variation occur in the original synthesized data (Tables 2 and 3). We therefore developed a methodology to understand the principal changes. We analyzed the different types and reclassifications of the grid cells according to the several-digit value to identify glacier retreat and advance areas. The four-digit value from each multi-temporal grid cell was used to differentiate between real glacier changes and noise during the observation period, caused by geo-location error (e.g. systematic error) or misclassifications (e.g. noise). The primary principles for distinguishing real glacier changes were based on characteristics of glacier dynamics, i.e., for a glacier near steady state it is unusual to retreat over the small distance of one or several pixels, then advance, then retreat again in years. The major affiliation principles were also applied in the detection and elimination of some noises.

Category 1: grid cells with a value of 5777 (Table 2, Fig. 3) (especially those at the glacier terminus or margin) represent the sequel "non-glacierized area → glacier area → glacier area → glacier area", i.e., a "non-glacierized area" at the first observation became a "glacier area" in the second observation, and remained a glacier area in the succeeding years. This was classified as "Glacier advance areas", where non-glacierized areas became glacier areas. A similar interpretation applies to the grid values 5577 and 5557, where glacier areas emerged later.

Table 2
Information table of the multi-temporal glacier change process in the Mt. Naimona'Nyi region (Grid cell area, 900 m^2).

Value of the multi-temporal grid unit	Count of grid units	Area (km^2)	Recode	Category of variation
5555	714,479	643.03	9	Non-glacierized area during 1976–2003
5557	120	0.11	3	Glacier advance area during 1999–2003
5575	1188	1.07	8	Noises in glacier area
5577	230	0.21	2	Glacier advance area during 1990–1999
5755	1494	1.34	8	Noises in glacier area
5757	266	0.24	8	Noises in glacier area
5775	824	0.74	8	Noises in glacier area
5777	2035	1.83	1	Glacier advance area during 1976–1990
7555	4659	4.19	4	Glacier retreat area during 1976–1990
7557	205	0.18	8	Noises in glacier area
7575	1371	1.23	8	Noises in glacier area
7577	706	0.64	7	Glacier area in stable termini during 1976–2003
7755	2091	1.88	5	Glacier retreat area during 1990–1999
7757	648	0.58	7	Glacier area in stable termini during 1976–2003
7775	3540	3.19	6	Glacier retreat area during 1999–2003
7777	82,141	73.93	7	Glacier area in stable termini during 1976–2003

Table 3
Information table of the multi-temporal grid on the glacier change process in the Mt. Qomolangma region.

Value of the multi-temporal grid unit	Recode	Area (km^2)	Category of variation
5555	9	135.783	Non-glacierized area during 1974–2003
5557	3	0.036	Glacier advance area during 2000–2003
5577	2	0.086	Glacier advance area during 1992–2000
5755	8	0.032	Noises in glacier area
5775	8	0.012	Noises in glacier area
5777	1	0.351	Glacier advance area during 1974–1992
7555	4	10.784	Glacier retreat area during 1974–1992
7557	8	0.013	Noises in glacier area
7577	7	0.001	Glacier area in stable termini during 1974–2003
7755	5	2.322	Glacier retreat area during 1992–2000
7757	7	0.018	Glacier area in stable termini during 1974–2003
7775	6	1.445	Glacier retreat area during 2000–2003
7777	7	129.060	Glacier area in stable termini during 1974–2003

Category 2: grid cells with values 7555, 7755 and 7775 (especially those at the glacier margin) were classified as "Glacier retreat areas", where glacier areas became non-glacierized areas during different periods. For example, grid cells value by 7555 represent grid cell variation by "glacier area → non-glacierized area → non-glacierized area → non-glacierized area", i.e., it was the "glacier area" at the first observation and became the "non-glacierized area" at the second observation, and remained the non-glacierized area in the succeeding years.

Category 3: grid cells where the hybrid values indicate changes that occur more rapidly than is considered possible (e.g. 5757, 7575, etc.) within a few years are considered as noise during the observation period in several decades.

Category 4: grid cells with three of the four digits being the same showed an agreement among three of the four values. Thus cells with values of 7757, 7577 were reclassified as the "stable glacier area", re-assigning these units by value 7777, whereas units with values 5575, 5755 were reclassified into the "stable non-glacierized area" and were re-assigned by value 5555. In this way, noise emerging from one of the four images could be removed.

Category 5: spatial neighborhood relationships were considered in glacier coverage changes. Grid cells with a value of 5775 indicate areas of variation on the "non-glacierized area → glacier area → glacier area → non-glacierized area" in the four periods. These areas of mainly rock ridges occurred in the high elevation area surrounded by glaciers in the accumulation zones, and not at the terminus or boundaries of glaciers (Fig. 4). Such areas that were misclassified due to snow cover could be distinguished with real glacier changes by interactive visualized maps of the multi-temporal grid data with neighborhood considerations.

Each category region could be identified by both visualization on maps (Figs. 3 and 4) and quantities in Tables 2 and 3. All glacier changes and identified noises led to adjusted data both in mapping (e.g. Fig. 4) and in quantity by the Reclass function using remap tables (e.g. Table 4) in the Arc/Info module with corrections of the misclassified grid cells.

4. Results

4.1. Study area 1: the Mt. Naimona'Nyi region

In the Mt. Naimona'Nyi region, the traditional method for quantifying classifications from individual images and maps in glacier monitoring showed that the area of glaciers coverage was 87.04 km^2 in 1976 and decreased to 79.39 km^2 in 2003 (Table 5). The rate of change varies during different periods. Recession was 2.59 km^2 during 1976–1990 (or 0.19 $km^2\ a^{-1}$ on average), 0.80 km^2 during 1990–1999 (or 0.09 $km^2\ a^{-1}$), and 4.27 km^2 during 1999–2003 (or 1.07 $km^2\ a^{-1}$). The total decrease in glacier area between 1976 and 2003 was equal to 7.66 km^2 or 8.8% (Table 6). Implementing the multi-temporal grid method we found

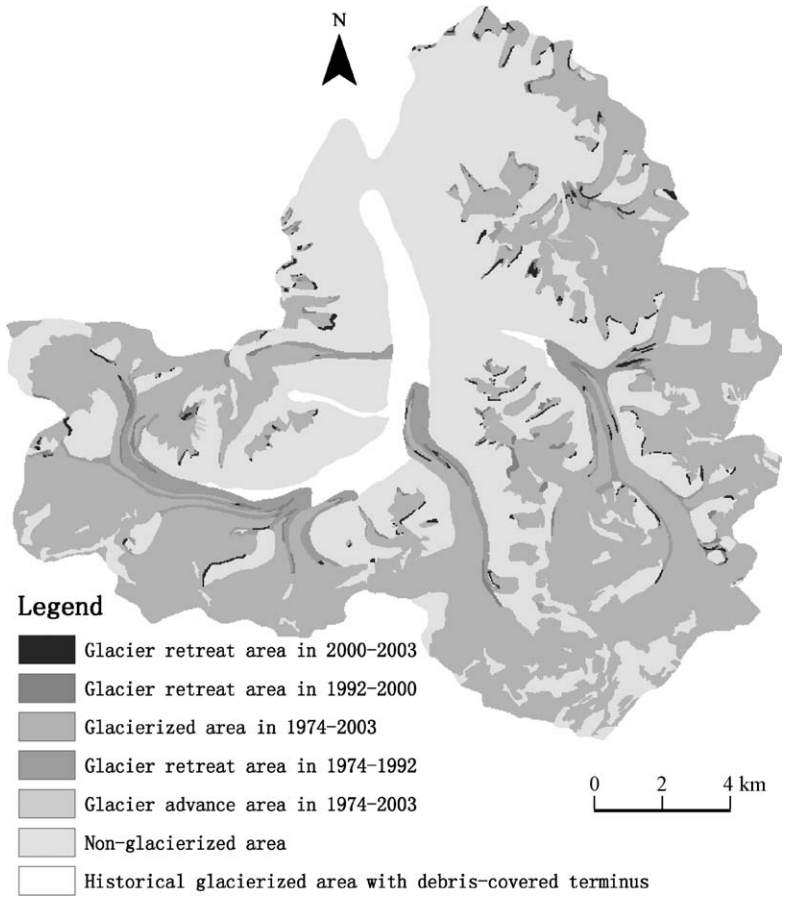

Fig. 4. Glacier coverage changes in the Mt. Qomolangma region during 1974–2003.

Table 4
Remap table of glacier changes by the multi-temporal grid in the Mt. Naimona'Nyi region.

Value of the multi-temporal grid unit	Recode	Area (km^2)	Category of variation
5777	1	1.83	Glacier advance area during 1976–1990
5577	2	0.21	Glacier advance area during 1990–1999
5557	3	0.11	Glacier advance area during 1999–2003
7555	4	4.19	Glacier retreat area during 1976–1990
7755	5	1.88	Glacier retreat area during 1990–1999
7775	6	3.19	Glacier retreat area during 1999–2003
7777, 7757, 7577	7	75.15	Glacier area in stable termini during 1976–2003
5757, 5775, 7557, 7575	8	2.40	Noises in glacier area
5555, 5575, 5755	9	645.44	Non-glacierized area during 1976–2003

discrepant grid cells of ever glacierized area by 4.81 km^2 (or 5.5% of the glacier area by 87.04 km^2 in 1976, including 2.41 km^2 or 2.77% grid units (by values of 5575 and 5755, Cat. 4) were reclassified as non-glacierized area and 2.4 km^2 or 2.76% grid cells (by value of 5757, 5775, 7557 and 7575, Cat. 3, Cat. 4 and Cat. 5) were identified as noises from glacier changes) were picked out and eliminated from glacier changes during 1976–2003. Further, 1.22 km^2 grid cells have been corrected into a stable glacier area, where grid cell values were equal to 7577, 7757 (Cat. 4, Table 2).

Differences in glacier changes in this region between the traditional method and the multi-temporal grid method are summarized in Table 5. After the noise removal from each individual classification, we notice that glacier recession clearly accelerates (Table 6). Recession was equal to 2.37 km^2 during 1976–1990 (or 0.17 $km^2\ a^{-1}$ on average), 1.67 km^2 during 1990–1999 (or 0.19 $km^2\ a^{-1}$ on average), and 3.08 km^2 during 1999–2003 (or 0.77 $km^2\ a^{-1}$ on average) (Fig. 3 and Table 6). The coverage of glaciers in this region was 84.41 km^2 in 1976 and 77.29 km^2 in 2003 (Table 5), showing a total decrease of 7.12 km^2, i.e., 8.44% or 0.31% a^{-1}, 0.26 $km^2\ a^{-1}$ (Table 6).

4.2. Study area 2: the Mt. Qomolangma region

In the Mt. Qomolangma region, the traditional method for quantifying classification results from individual images and maps in glacier monitoring showed that the glacier coverage was 144.64 km^2 in 1974 and decreased to

Table 5
Glacier area in different periods in the Mt. Naimona'Nyi region during 1976–2003.

Year	Area by common method (km^2)	Area by multi-temporal grid method (km^2)	Area difference (km^2)	Percentage of noises (%)	Value of the multi-temporal grid unit
1976	87.04	84.41	2.63	3.02	7777, 7757, 7577, 7555, 7755, 7775
1990	84.46	82.04	2.42	2.87	7777, 7757, 7577, 7755, 7775, 5777
1999	83.66	80.37	3.29	3.93	7777, 7757, 7577, 7775, 5577, 5777
2003	79.39	77.29	2.1	2.65	7777, 7757, 7577, 5557, 5577, 5777

Table 6
Glacier area change in the Mt. Naimona'Nyi region during 1976–2003 with results by the common method in the parentheses.

Periods	Variation in area (km^2)	Variation rate (%)	Annual variation rate (% a^{-1})	Annual variation (km^2 a^{-1})
1976–1990	−2.37 (−2.59)	−2.81 (−2.97)	−0.20 (−0.21)	−0.17 (−0.19)
1990–1999	−1.67 (−0.80)	−2.04 (−0.95)	−0.23 (−0.11)	−0.19 (−0.09)
1999–2003	−3.08 (−4.27)	−3.83 (−5.10)	−0.96 (−1.28)	−0.77 (−1.07)
Total	−7.12 (−7.66)	−8.44 (−8.80)	−0.31 (−0.38)	−0.26 (−0.28)

Table 7
Glacier area in different periods in the Mt. Qomolangma region during 1974–2003.

Year	Area by common method (km^2)	Area by the multi-temporal grid method (km^2)	Area difference (km^2)	Percentage of noises (%)	Value of the multi-temporal grid unit (remap table)
1974	143.64	143.63	0.01	0.01	7777, 7757, 7577, 7775, 7755, 7555
1992	133.24	133.20	0.04	0.03	7777, 7757, 7577, 7755, 7775, 5777
2000	130.96	130.96	0.00	0.00	7777, 7757, 7577, 7775, 5577, 5777
2003	129.57	129.55	0.02	0.01	7777, 7757, 7577, 5557, 5577, 5777

Table 8
Remap table of glacier changes by the multi-temporal grid in the Mt. Qomolangma region.

Value of the multi-temporal grid unit	Recode	Area (km^2)	Category of variation
5777	1	0.35	Glacier advance area during 1974–1992
5577	2	0.09	Glacier advance area during 1992–2000
5557	3	0.04	Glacier advance area during 2000–2003
7555	4	10.78	Glacier retreat area during 1974–1992
7755	5	2.32	Glacier retreat area during 1992–2000
7775	6	1.45	Glacier retreat area during 2000–2003
7777, 7757, 7577	7	129.08	Glacier area in stable termini during 1974–2003
5775, 7557	8	0.02	Noises in glacier area
5555, 5755	9	135.82	Non-glacierized area during 1974–2003

129.57 km^2 in 2003 (Table 7). By the multi-temporal grid method, grid units with values equal to 5755, 5775 and 7557 (Cat. 3, Cat. 4 and Cat. 5) that were ever "glacierized" areas total 0.06 km^2 or 0.04% of the total glacier coverage in 1974, could be identified as noise from glacier change results during 1974–2003 (Table 3). In addition, grid cells with values equal to 7577, 7757 (Cat. 4), totaling a 0.02 km^2, were reclassified into a stable glacier area (Table 3). Differences in glacier area from the two methods are summarized in Table 7. Noise removal from each

Table 9
Glacier variation in the Mt. Qomolangma region during 1974–2003 with results by common method in the parentheses.

Year	Variation in area (km^2)	Variation rate (%)	Annual variation rate (% a^{-1})	Annual variation (km^2 a^{-1})
1974–1992	−10.43 (−10.40)	−7.26 (7.24)	−0.40 (0.40)	−0.58 (−0.58)
1992–2000	−2.24 (−2.29)	−1.68 (1.72)	−0.21 (0.21)	−0.28 (−0.29)
2000–2003	−1.41 (−1.39)	−1.08 (1.06)	−0.36 (0.35)	−0.47 (−0.46)
Total	−14.08 (−14.08)	−9.80 (9.80)	−0.34 (0.34)	−0.49 (−0.49)

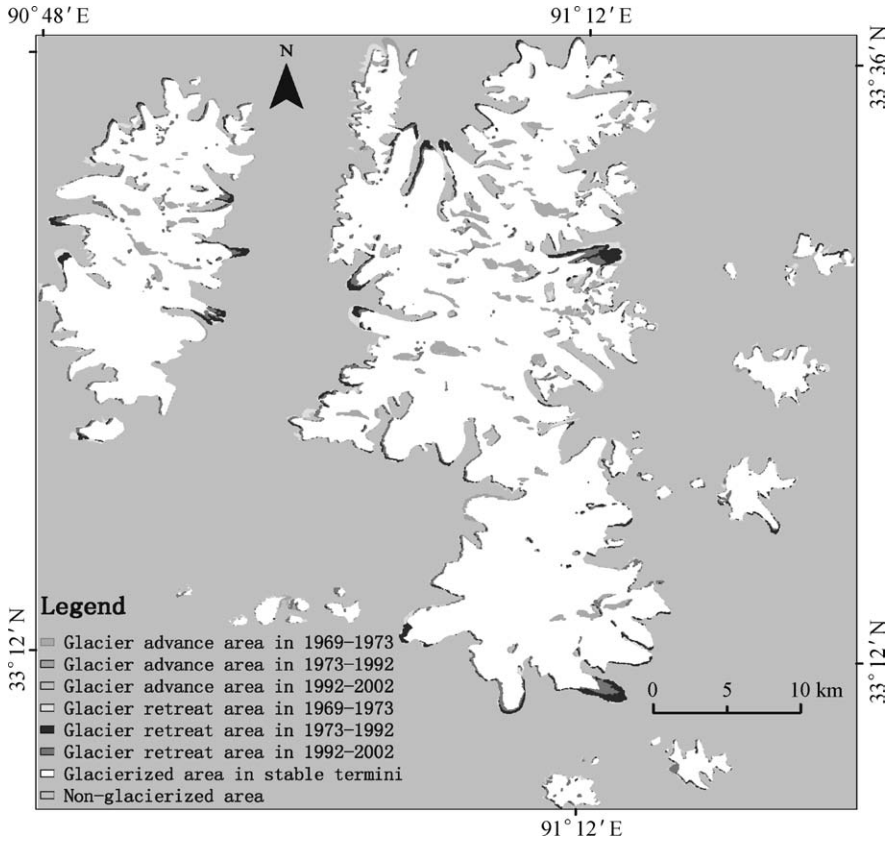

Fig. 5. Glacier coverage changes in the Mt. Geladandong region in 1969–2002.

individual data set did not substantially affect the results of the change trend, where glacier recession was clearly accelerated in recent years (Table 9). The total glacier recession in this region was 14.08 km^2, i.e., 9.8% or 0.34% a^{-1}, 0.49 km^2 a^{-1} during 1974–2003.

Noise from individual data sets by manual digitization in this region was smaller than that by band algorithms found in the Mt. Naimona'Nyi region (Table 5). The largest coverage variation occurred during 1974–1992, showing a glacier recession of approximately 10 km^2, or 0.4% a^{-1}. The results were derived from different data sources, the topographic maps in 1974 and the Landsat/TM image in 1992.

Apparently, inconsistencies increase largely if non-satellite data such as aerial photography, topographic maps and historical digitized maps are included, e.g. this also resulted in large discrepancies in the "Glacier advance area during 1969–1973" in the Mt. Geladandong region, the blue area in Fig. 5, which totaled 27.66 km^2 or 3.4% of the stable glaciers.

Glaciers in the Mt. Naimona'Nyi region and in the Mt. Qomolangma region both increased and decreased during the research period (Tables 4 and 8). However, the glacier retreat area was much larger than that of the glacier advance area (Tables 4 and 7). The glacier advance area decreased through time, whereas the retreated area increased in recent years.

5. Discussion

Comparing the results from the multi-temporal grid method with that obtained by a traditional method (Tables 5 and 7), we found that the multi-temporal grid method allowed us to reduce impropriate variation in glacier distribution caused by using different sensors, geo-location errors, or misclassification. We also notice that manual digitization results in much less noise and discrepancies than an automatic bands algorithms method with operations between multiple bands, e.g. band ration. Our final results, however, may still incorporate some of these factors and further research may be appropriate here.

5.1. Measurement noise

Grid cells of non-glacierized areas in the mountains derived from the earlier images or topographic maps (e.g. at the 1:50,000 or 1:100,000 scale) that were absent on the later sequential images, could have resulted in an overestimation of the Glacier advance area in the later period. For example, the grid cells with value equal to 5777 (classified as Cat. 1) in Fig. 3 represent the "glacier advance area during 1976–1990" in the Mt. Naimona'Nyi region. Most of these, however, are artifacts and do not correspond to real glacier advance. A similar interpretation holds for the grey area in mountains shown in Fig. 5,

where, approximately 50 km^2 of discrepancies would exist in glacier changes, covering 5.6% of the total glacier area in the 1969 topographic maps in the Mt. Geladandong region, if those grid cells were also regarded as noise. Therefore, some grid cells with a value equal to 5777 should be reclassified as discrepancies both in the Mt. Naimona'Nyi and in Mt. Geladandong regions. Such noise, however, could not be corrected by using a remap table as some gridcells with a value of 5777 represent real glacier advances or ice movements during that period.

Misclassifications of the non-glacierized areas as glaciers in the earlier maps or images, may also have resulted in an overestimation of glacier retreat during the corresponding period. For example, the smaller remaining "noise" in the Mt. Naimona'Nyi region shown in Fig. 3, originates from non-glacierized areas surrounded by glacier areas, but not at the glacier termini, such as high mountain rock ridges, rock outcrops, and steep mountain peaks, which were misidentified as glacierized areas from earlier data (i.e., the 1999 image). They were, however, correctly identified as non-glacierized areas in the 2003 image. These discrepancies could be identified by the multi-temporal grid method using the neighborhood relationship considerations and corrected in the individual classification results according to the corresponding images further. Differences in handling rock outcrops are another source of difference [21].

5.2. Measurement uncertainty

Measurement uncertainty emerges as the accuracy of the position of the glacier front identified by remote sensing images and is limited by both the sensor resolution [1] and the co-registration error [13,36]. Calculated by the sensor resolution and co-registration error [38], the maximum measurement uncertainty in the coverage of glaciers was approximately 0.015 km^2 in the Mt. Naimona'Nyi region, 0.044 km^2 in the Mt. Qomolangma region, and 0.042 km^2 in the Mt. Geladandong region. Using the multi-temporal grid method, however, we eliminated more than 2.5 km^2 of noise or 3.0% of the total glacier coverage in 1976 from classification results in the Mt. Naimona'Nyi region (Table 4). Similarly, corrections of approximately 22.4 km^2 of noise or 2.5% of the total glacier coverage by 889.3 km^2 in 1969 were made for the Mt. Geladandong region. In the Mt. Qomolangma region, 0.06 km^2 or 0.04% of the total glacier coverage in 1974 was identified as noise from glacier change results during 1974–2003. Such noise among sequential data sets was much higher than that of the measurement uncertainty by sensor resolution and co-registration error. Therefore, uncertainty in glacier monitoring by satellite images mainly originates from such noise in sequential data sets, caused by geo-location error or misclassifications.

5.3. Future work

Not all identified discrepancies or noise in the maps could be corrected by the multi-temporal grid method without further study or verification, for example, the 5777 (Cat. 1) area in the Mt. Naimona'Nyi and Mt. Geladandong regions (e.g. Fig. 5). Those problematic areas could be further reduced by the knowledge of glaciologists or field surveys. A proper validation would depend upon physical features of the research objects, actual information, different data interpretations, research experience, and expert knowledge.

The multi-temporal grid method may work as well for debris-covered glaciers to detect noise in individually interpreted results from multi-temporal images with local experience or field survey. It may not work, however, for classification and delineation of debris-covered glaciers from multi-spectral satellite images. Therefore, in this paper, we only studied clean glaciers in the Himalayas.

Our results quantify the areas of both glacier retreat and advance in the middle and western Himalaya Mountains. Retreat dominates and accelerates through time in the two regions. The retreat is due to the negative glacier mass balance and is affected by rising air temperatures over the Tibetan Plateau [31]. Glacier variation in the two regions also shows spatial differences. Retreat occurs in the southeast facing glaciers, whereas advances occur in the northwest facing glaciers. The causes for advance of some glaciers in the two regions, however, have not been identified because of the paucity of field survey and regional meteorological data. Furthermore, this work focused on variation in glacier coverage and did not include height variation. In the future, we will study glacier volume changes by high resolution satellite stereo pair images (e.g. stereo pair data from ASTER, ALOS/PRISM or SPOT), or by the high resolution vertical change detector LIDAR (Light Detection And Ranging) or by InSAR techniques, then evaluate their uncertainties by *in-situ* field surveyed measurements in the two regions, which will enable us to generate a more comprehensive view of glacier changes in the Mt. Naimona'Nyi region and the Mt. Qomolangma region of the Himalayas.

6. Conclusions

This paper describes a multi-temporal grid method for studying glacier changes by remote sensing and GIS. It compares the results from two different methods and provides a detailed visualization of glacier changes in each epoch. The multi-temporal grid method distinguishes between noise due to geo-location noise and misclassifications from real glacier changes occurring over periods of decades. It detects and eliminates discrepancies (e.g. by 3.0% of the total glacier coverage in 1976 from classification results in the Mt. Naimona'Nyi region) based on algebraic operations within grid cells. The comparison of this method with a traditional method demonstrates an improvement in quantifying glacier variation. The identified discrepancies or noise (e.g. by 2.5 km^2 in the Mt. Naimona'Nyi region) is much larger than that of the measurement uncertainty limited by sensor resolution and

co-registration error (e.g. by 0.015 km^2 in the Mt. Naimona'Nyi region). This may affect the way in calculation of measurement uncertainty in glacier change monitoring by satellite imagery. Not all detected noise, however, could be corrected by this method without further study or verification by field survey.

Results obtained in this study show that areas of both glacier retreat and advance exist in the middle and western Himalayas with retreat dominating and accelerating. Glaciers on the northern slope of Mt. Qomolangma in the middle Himalayas retreat more extensively and faster than that in the western Himalayas in the Mt. Naimona'Nyi region. The 0.34% a^{-1} retreat of the total glacier area or in the Qomolangma region during 1974–2003 was larger than the 0.31% a^{-1} retreat in the Mt. Naimona'Nyi region during 1976–2003, both of them are larger than the average 0.175% a^{-1} retreat of glaciers in high Asia in the last 40 years since the 1960s [31] and the 0.18% a^{-1} area loss in the Mt. Geladandong region in Central Tibet during 1969–2002.

We conclude that the multi-temporal grid method gives important and novel opportunities when analyzing changes in glacier coverage in the Tibetan Plateau. Clear differences between the studied glaciers were apparent, pointing to possibly different mechanisms of change.

Acknowledgements

The work was supported by the National Natural Science Foundation of China (40601056 and 40121101), the Special Science Foundation on Meteorological Project Research for Public Benefit (GYHY(QX)2007-6-18), the Opening Fund Projects of State Key Laboratory of Remote Sensing Science in the Institute of Remote Sensing Applications, the Innovative Project of Institute of Tibetan Plateau Research (ITPR), CAS and through a cooperation project between the Climate Change Institute, University of Maine supported by the National Oceanic and Atmospheric Administration (NA04OAR4600179) and the Institute of Tibetan Plateau Research (ITPR), CAS. The authors thank Susan Kaspari, Paul A. Mayewski, Gordon Hamilton and Andrei Kurbatov for their helpful suggestions on the paper. Special thanks are given to Richard S. Williams, Jr., three anonymous reviewers and Dr. Marvin E. Bauer for their helpful comments and great efforts on the paper.

References

[1] Williams Jr RS, Hall DK, Sigurdsson O, et al. Comparison of satellite-derived with ground-based measurements of the fluctuations of the margins of Vatnajökull, Iceland, 1973–1992. Ann Glaciol 1997;24:72–80.

[2] Bindschadler R, Dowdeswell J, Hall D, et al. Glaciological applications with Landsat-7 imagery: early assessments. Remote Sens Environ 2001;78:163–79.

[3] Williams Jr RS, Ferrigno JG. Satellite image atlas of glaciers of the world: U.S. geological survey fact sheet fs-2005–3056; 2005. Available from: http://www.pubs.usgs.gov/fs/2005/3056/fs2005-3056.pdf or http://www.glaciers.er.usgs.gov/.

[4] Meier MF. Evaluation of ERTS imagery for mapping and detection of changes in snow cover on land and on glaciers. In: Symposium on significant results obtained from the earth resources technology satellite-1. Washington, DC: NASA, USA; 1973. p. 863–75.

[5] Kääb A. Monitoring high-mountain terrain deformation from repeated air- and spaceborne optical data: examples using digital aerial imagery and ASTER data. ISPRS J Photogramm 2002;57:39–52.

[6] Bishop MP, Barry RG, Bush ABG, et al. Global land ice measurements from space (GLIMS): Remote sensing and GIS investigations of the Earth's Cryosphere. Geocarto Int 2004;19(2):57–84.

[7] Kargel J, Abrams MJ, Bishop MP, et al. Multispectral imaging contributions to global land ice measurements from space. Remote Sens Environ 2005;99(1–2):187–219.

[8] Raup B, Kääb A, Kargel JS, et al. Remote sensing and GIS technology in the Global Land Ice Measurements from Space (GLIMS) Project. Comput Geosci 2007;33(1):104–25.

[9] Raup BH, Kieffer HH, Hare TM, et al. Generation of data acquisition requests for the ASTER satellite instrument for monitoring a globally distributed target: glaciers. IEEE T Geosci Remote 2000;38(2):1–9.

[10] Khalsa SJS, Dyurgerov MB, Khromova T, et al. Space-based mapping of glacier changes using ASTER and GIS tools. IEEE T Geosci Remote 2004;42(10):2177–82.

[11] Khromova TE, Osipova GB, Tsvetkov DG, et al. Changes in glacier extent in the eastern Pamir, Central Asia, determined from historical data and ASTER imagery. Remote Sens Environ 2006;102:24–32.

[12] Hall DK, Chang ATC, Foster JL, et al. Comparison of in-situ and Landsat reflectance of Alaskan glaciers. Remote Sens Environ 1989;28:23–31.

[13] Silverio W, Jaquet JM. Glacial cover mapping (1987–1996) of the Cordillera Blanca (Peru) using satellite imagery. Remote Sens Environ 2005;95:342–50.

[14] Holben BN, Justice CO. An examination of spectral band ratioing to reduce the topographic effect on remotely sensed data. Int J Remote Sens 1981;2(2):115–33.

[15] Bayr KJ, Hall DK, Kovalick WM. Observations on glaciers in the eastern Austrian Alps using satellite data. Int J Remote Sens 1994;15:1733–42.

[16] Jacobs JD, Simms EL, Simms A. Recession of the southern part of Barnes Ice Cap, Baffin Island, Canada, between 1961 and 1993, determined from digital mapping of Landsat TM. J Glaciol 1997;43:98–102.

[17] Paul F. Evaluation of different methods for glacier mapping using Landsat TM. EARSeL eProc 2001;1:239–45.

[18] Paul F, Kääb A, Maisch M, et al. The new remote-sensing-derived Swiss glacier inventory: I. Methods. Ann Glaciol 2002;34:355–61.

[19] Kääb A, Manley B, Paul F, et al. GLIMS algorithm document from GLIMS Algorithm Working Group; 2006. Available from: http://www.geo.unizh.ch/kaeaeb/glims/algor.html#Anchor-23240.

[20] Kääb A. Combination of SRTM3 and repeat ASTER data for deriving alpine glacier flow velocities in the Bhutan Himalaya. Remote Sens Environ 2005;94:463–74.

[21] Raup B, Racoviteanu A, Khalsa SJS, et al. The GLIMS geospatial glacier database: a new tool for studying glacier change. Global Planet Change 2007;56(1–2):101–10.

[22] Kuzmichenok V, Aizen N, Surazakov A, et al. Assessment of glacial area and volume change in Tien Shan (Central Asia) during the last 60 years using geodetic, aerial photo, ASTER and STRM data. In: Abstracts of 2004 AGU Fall Meeting. Eos Trans (Suppl.) 2004;85(47):F110.

[23] Mayewski PA, Jeschke PA. Himalayan and trans-Himalayan glacier fluctuations since A.D. 1812. Arct Antarct Alp Res 1979;11(3):267–87.

[24] Miller KJ, editor. The International Karakoram Project. In: Proceedings of the international conference. Cambridge: Cambridge University Press; 1984.

[25] Chen J, Liu C, Jin M. Application of the repeated aerial photogrammetry to monitoring glacier variation in the drainage area of the Urumqi River. J Glaciol Geocryol 1996;18(4):331–6, [in Chinese].
[26] Li Z, Sun WX, Zeng Q. Measurements of glacier variation in the Tibetan Plateau using Landsat data. Remote Sens Environ 1998;63:258–64.
[27] Wang Z, Liu C. Geographical characteristics of the distribution of glaciers in China. J Glaciol Geocryol 2001;23(3):231–7, [in Chinese].
[28] Pu JC, Yao TD, Wang N, et al. Recent variation of Malan glacier in Hoh Xil Region, Center of Tibetan Plateau. J Glaciol Geocryol 2001;23(2):189–92, [in Chinese].
[29] Liu SY, Shen YP, Sun WX, et al. Glacier variation since the maximum of the little ice age in the western Qilian Mountains, Northwest China. J Glaciol Geocryol 2002;24(3):227–33, [in Chinese].
[30] Lu AX, Yao TD, Liu SY, et al. Glacier change in the Geladangdong area of the Tibetan Plateau monitored by remote sensing. J Glaciol Geocryol 2002;24(5):559–62, [in Chinese].
[31] Yao TD, Wang YQ, Liu SY, et al. Recent glacial retreat in High Asia in China and its impact on water resource in Northwest China. Sci China Ser D 2004;47(12):1065–75.
[32] Fujita K, Thompson LG, Ageta Y, et al. Thirty-year history of glacier melting in the Nepal Himalayas. J Geophys Res 2006;111(D03109). doi: 10.1029/2005JD005894.
[33] Ye QH, Chen F, Yao TD, et al. Tupu of glacier changes in the Mt. Naimona'Nyi Region, Western Himalayas, in the last three decades. J Remote Sens 2007;11(4):511–20, [in Chinese].
[34] Xie ZC, Su Z. Glacier development, quantity and distribution on the northern slope. In: Report on the scientific expedition to the Mt. Everest in 1966–1968, modern glacier and landforms. Beijing: Sci Press; 1975. p. 92–105, [in Chinese].
[35] Kang SC, Mayewsk PA, Qin DH. Glaciochemical records from a Mt. Everest ice core: Relationship to atmospheric circulation over Asia. Atmos Environ 2002;36(21):335l–61.
[36] Hall DK, Bayr KJ, Schöner W, et al. Consideration of the errors inherent in mapping historical glacier positions in Austria from the ground and space (1893–2001). Remote Sens Environ 2003;86:566–77.
[37] Ye QH, Yao TD, Kang SC, et al. Glacier changes in the Mt. Naimona'Nyi Region, Western Himalayas, in the last three decades. Ann Glaciol 2006;43:385–9.
[38] Ye QH, Kang SC, Chen F, et al. Monitoring glacier changes on Geladandong mountain, central Tibetan Plateau, from 1969 to 2002 using remote-sensing and GIS technologies. J Glaciol 2006;52(179):537–45.
[39] Chen SP. A preliminary discussion on conception of geo-informeta-map (Tupu) design. Geograph Res 1998;17(Suppl.):5–10, [in Chinese].
[40] Chen SP, Yue TX, Li HG. Studies on geo-informatic Tupu and its applications. Geograph Res 2000;19(4):337–43, [in Chinese].
[41] Chen SP. Primarily research of Geo-information Tupu. Beijing: Business Press; 2001, [in Chinese].
[42] Ye QH, Liu GH, Tian GL, et al. Geospatial–temporal analysis of land-use changes in the Yellow River Delta in the last 40 years. Sci China Ser D 2004;47(11):1008–24.